ACS Catalysis

pubs.acs.org/acscatalysis

Research Article

Using Transient XAS to Detect Minute Levels of Reversible S-O Exchange at the Active Sites of MoS_2-Based Hydrotreating Catalysts: Effect of Metal Loading, Promotion, Temperature, and Oxygenate Reactant

Abhijeet Gaur,* Matthias Stehle, Marc-André Serrer, Magnus Zingler Stummann, Camille La Fontaine, Valérie Briois, Jan-Dierk Grunwaldt, and Martin Høj*

Cite This: *ACS Catal.* 2022, 12, 633−647

Read Online

ACCESS | Metrics & More | Article Recommendations | Supporting Information

ABSTRACT: Modulation excitation spectroscopy (MES) coupled with time-resolved X-ray absorption spectroscopy (XAS) was applied to unpromoted and Co-promoted Mo-based hydrotreating catalysts (*i.e.*, Mo and CoMo catalysts) for investigating the minute as well as instantaneous differences in active site composition under the influence of H_2S and H_2O. Transient experiments during alternating sulfur- and water-rich conditions were performed at temperatures between 400 and 500 °C using catalysts with varying Co/Mo metal loadings to study the correlative effect of these factors on the stability of the active sites. For both types of catalysts, the features of the demodulated Mo K-edge spectrum matching the difference spectra of the MoS_2 and MoO_3 references indicate a reversible oxidation−sulfidation process during H_2O/H_2S cycling. In the case of CoMo catalysts with increasing metal loadings, transient XAS at the Mo K- as well as Co K-edge revealed minute levels of S-O exchange at both sulfided Mo and Co sites, although 26 to 47% of the Co was bound as stable $CoAl_2O_4$, which does not form a bulk sulfide. Thus, even in the presence of multiple Co phases (oxide and sulfide) and a low number of active sites relative to the total number of Mo atoms, transient XAS can successfully detect the changes occurring over both the active Co and Mo sites. Furthermore, the comparison of the amplitude of the demodulated spectra showed that Mo atoms are more prone to S-O exchange with increasing temperature, while Co promotion stabilized the molybdenum sulfide. MES-coupled XAS experiments with 1-propanol performed to evaluate the degree of S-O exchange in the presence of another oxygenate reactant revealed the higher affinity of water toward these sulfided Mo sites as compared to 1-propanol.

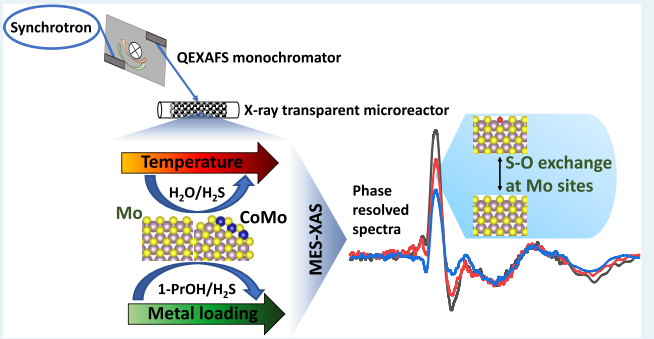

KEYWORDS: *hydrodeoxygenation, Mo sulfide catalyst, CoMo catalyst, transient XAS, EXAFS, modulation excitation spectroscopy, surface sensitivity*

1. INTRODUCTION

Sulfided CoMo, NiMo, and Mo catalysts are industrially used for hydrotreating crude oil due to their moderate costs and inherent sulfur tolerant nature as compared to most reduced metal catalysts.[1,2] The catalysts are also active for hydrodeoxygenation (HDO) of bio-oil and oxygenate model compounds, showing promising activity and stability.[3−8] Recently, it has been reported that these catalysts are also used industrially for HDO of renewable feeds such as used cooking oil and animal fat.[9] Addition of a promoter (Co or Ni) to MoS_2 leads to enhanced deoxygenation activity due to increased formation of coordinatively unsaturated sites.[10,11] Furthermore, the state of the active sites is strongly influenced by the H_2O/H_2S ratio. By maintaining the optimal H_2O/H_2S ratio, S-O exchanges that lead to deactivation of active sulfided Mo sites can be avoided. In order to optimize sulfided catalysts for HDO, the influence of H_2S and H_2O were thoroughly investigated experimentally in a previous study, both in terms of HDO activity and catalyst structure.[5] The active sites of Co-MoS_2 and Ni-MoS_2 catalysts are located at the edges and corners of MoS_2 nanoparticles and, thus, only constitute a small fraction of all Mo atoms in the catalyst.[12,13] However, further characterization is needed to unravel the actual structure and composition of the catalytically active sites

Received: October 15, 2021
Revised: December 5, 2021
Published: December 23, 2021

relevant for HDO, especially under realistic reaction conditions. This requires the use of techniques that are sensitive enough to detect minute changes relative to the bulk MoS_2.[14]

Recently, Stummann *et al.*[15] have investigated these HDO catalysts to study the effect of CoMo loading and support acidity on the product distribution and deoxygenation activity in catalytic hydropyrolysis of biomass. Detailed understanding of the effect of catalyst properties on product selectivity has been obtained by characterizing the calcined oxide precursors with Raman spectroscopy, temperature-programmed desorption of ammonia (NH_3-TPD), and N_2 physisorption (BET method). Further, the spent catalysts were characterized with electron microscopy (SEM and STEM). It has been shown that by increasing the CoMo loading and/or changing the support acidity, it was possible to decrease the oxygen content in the organic phase while maintaining a high yield.

In another study, Plais *et al.*[16] have used Co K-edge quick-X-ray absorption spectroscopy (quick-XAS) combined with multivariate analysis to study the sulfidation pathways under a 10% H_2S/H_2 atmosphere for oxidic cobalt species supported on alumina and silica. A transformation of oxidic cobalt species into nanometer-sized CoS_2 particles was observed before the final conversion into nanometer-sized Co_9S_8 particles. It has been concluded that the smaller the size of the Co_9S_8 nanoparticles, the higher the amount of formed CoS_2 after cooling under a sulfiding atmosphere. Further, the quantification of the CoMoS active species has been performed *in situ* during the sulfidation of a calcined Co-promoted MoS_2-based HDS catalyst by using the column-wise augmented strategy in multivariate curve regression with alternating least square (MCR-ALS) analysis.

For unpromoted and Co/Ni-promoted MoS_2-based HDO catalysts, Dabros *et al.*[5] have reported DFT studies, catalytic activity tests, and *in situ* XAS to provide detailed information on the activity and stability of these catalysts upon variation of the partial pressures of H_2O and H_2S. DFT calculations showed that the active edge of MoS_2 could be stabilized against S-O exchanges by increasing the partial pressure of H_2S or by promotion with either Ni or Co. The evolution of the active sulfide phase of the catalysts and the influence of varying H_2O/H_2S ratios on the catalyst structure have been studied *in situ* with XAS showing that the catalysts were tolerant toward water and that the active phases were present as small and highly dispersed particles.

Dynamic conditions of temperature, pressure, gas atmosphere, *etc.*, can cause chemical transformation of the catalysts, specifically changes to the surface composition while the bulk structure remains the same. Thus, complementary techniques are required for detailed studies of the structural, electronic, and chemical properties of catalysts under dynamic reaction conditions. X-ray absorption spectroscopy (XAS) is an element-specific technique, and due to the high penetration of hard X-rays through the reactor and the catalyst bed, it can probe the state of a catalyst under working conditions.[17,18] However, the sensitivity of XAS toward minority species is usually very low, as it is probing the bulk. In such cases, the combination of XAS with modulation excitation spectroscopy (MES) under transient experimental conditions (*e.g.*, type and concentration of reactants or temperature) can be used to separate the spectroscopic signals from active species undergoing transformation from the spectator species.[19] MES is used in combination with a variety of time-resolved spectroscopic techniques such as XAS, X-ray diffraction (XRD), infrared (IR), and Raman spectroscopy.[19−24] MES analysis exclusively provides signals from species responding to the external stimulation, which makes it possible to extract signals from these minority species that are otherwise difficult to observe.[14,24−26] Thus, the combination of XAS with MES[27] has been helpful to understand the catalytic process by providing chemical, structural, and electronic insights into the catalysts and other involved species.

In a recent study, Serrer et al.[28] have used XAS-coupled MES to study the role of iron in bimetallic Ni−Fe catalysts during CO_2 methanation. By enhancing the surface sensitivity of XAS with MES, it was observed that Fe shows a highly dynamic behavior during CO_2 activation. It was proposed that an $Fe^0 \rightleftharpoons Fe^{2+} \rightleftharpoons Fe^{3+}$ redox cycle, highly likely located at the interface between FeO_x clusters and the surface of the metal particles, promotes CO_2 dissociation during the methanation reaction. Lately, Czioska et al.[29] have studied the IrO_2-catalyzed oxygen evolution reaction (OER) at various potentials by employing conventional *operando* and MES-XAS measurements for understanding the different mechanisms that occur during OER. By using difference spectra and FEFF9 calculations, two different OER modes were assigned that took place in the uncalcined as well as in the calcined samples. MES-XAS unraveled that these modes could be assigned to a modification in the role of oxygen vacancies in the mechanism when switching from low to high OER potentials.

In an earlier work,[14] we have studied a MoS_2-based HDO catalyst by employing XAS-coupled MES where the catalytic system was modulated by periodically alternating between H_2O/H_2 and H_2S/H_2 conditions while the spectra were acquired continuously. By employing MES-XAS for unpromoted as well as Co- and Ni-promoted MoS_2 catalysts, it was concluded that O atoms replace S atoms at the edges of MoS_2 during H_2O exposure. The extent of S-O exchange was reduced for promoted catalysts, indicating the positive effect of promotion on catalytic activity.

In the present work, in order to examine the effect of various factors on the stability and activity of the HDO catalysts, we report a detailed MES coupled time-resolved XAS study on Co promoted and unpromoted MoS_2 catalysts. This study provides an experimental environment for measuring dynamic changes to the active site composition under the influence of H_2S and H_2O or 1-propanol. Co-promoted MoS_2 catalysts having varying metal loadings were investigated at the Co K- and Mo K-edges, and experiments were performed at different temperatures (400, 450, and 500 °C) under H_2O/H_2S or 1-propanol/H_2S cycling to study the effect of temperature, oxygenate reactant, metal loading, and promotion on the stability of the active sites. The obtained results were discussed to explain the changes taking place on catalyst surfaces and also to compare the degree of these changes due to the variation in reaction conditions.

2. EXPERIMENTAL SECTION

2.1. Catalysts Preparation. The catalysts were prepared by incipient wetness impregnation using $MgAl_2O_4$ (supplied by Haldor Topsøe) as the support material. The precursors used for the preparation were $(NH_4)_6Mo_7O_{24}\cdot 4H_2O$ (Fluka ≥99.0%) for Mo and $Co(NO_3)_2\cdot 6H_2O$ (Fluka ≥98%) for Co. After impregnation with Mo, the catalyst was dried overnight at 110 °C before it was impregnated with Co. The

https://doi.org/10.1021/acscatal.1c04767
ACS Catal. 2022, 12, 633−647

catalysts were then calcined under an air flow of 1.24−1.30 NL/min technical air (20% O_2 in N_2) at 500 °C (ramp: 5 °C/min) and holding for 3 h.[15] The calcined catalysts were sieved to 180−355 μm to remove any agglomerates or dust formed during the catalyst preparation. The elemental composition and the specific surface area (BET method) of the calcined CoMo catalysts after impregnation are given in Table 1.

Table 1. Metal Loading, Co/Mo-Ratio, and Specific Surface Area of the CoMo Catalysts after Calcination

sample	Co loading (wt %)	Mo loading (wt %)	Co/Mo ratio (molar)	specific surface area (m^2/g)
CoMo 1	0.64	3.4	0.30	60
CoMo 2	1.49	7.7	0.31	136
CoMo 3	1.86	10.1	0.31	148

2.2. X-Ray Absorption Spectroscopy (XAS) Data Acquisition. Time-resolved quick-XAS[30] data were recorded at the ROCK beamline,[31] SOLEIL synchrotron. For this purpose, the quick-EXAFS (QEXAFS) method with recording XAS data "on the fly"[30,32] was used based on a cam-driven tilt table on which the channel-cut is installed.[33] The beamline is equipped with two independent channel-cut monochromators (Si(111) and Si(220)) and a remotely controlled automation for exchanging optics and detectors (Okken ionization chambers).[34] By this, fast switches between the edge positions of the different metals were facilitated to monitor quasi-simultaneous structural changes in the reactor, *i.e.,* changes at the Mo K-edge and Co K-edge. The oscillation frequency of the monochromators was fixed at 2 Hz, leading to a spectrum acquisition with increasing Bragg angles every 250 ms. Taking advantage of the small beam size of X-rays (typically 0.5 mm (H) × 0.3 mm (V)) at the focusing position at the ROCK beamline, for the MES experiments involving 1-propanol, the spectra were measured alternately at the inlet as well as at the outlet position of the quartz microreactor to compare the state of the catalyst along the fixed bed. For MES experiments involving H_2O, spectra were measured at the middle of the catalytic bed. Details of the setup employed for the *in situ* XAS-coupled MES experiments are given in an earlier study.[14] For the *in situ* experiments, 7 mg catalyst was loaded into a 1.0 mm-diameter quartz capillary[17] with a wall thickness of 0.02 mm. Figure 1 shows an overview of the different steps performed during MES experiments. The oxide catalyst precursor was first dehydrated and then converted to the active sulfide form by treating it under a flow of 10% H_2S/H_2 (25−35 NmL/min) and heating to 400 °C with a holding time of 30 min at the target temperature. In the next step, a pneumatic four-way valve was used to perform the MES experiments by cycling between 3% H_2O/H_2 (1st cycle, 180 s) and 500 ppm H_2S/H_2 (2nd cycle, 180 s) with a total period of 360 s. XAS spectra for CoMo samples have been recorded in transmission mode using the alternate measurement of Co and Mo K-edges during the *in situ* sulfidation step. Single edge acquisition was performed during the MES step. For collection and initial processing of the spectra, a graphical user interface (GUI, developed at SOLEIL) dedicated to the data obtained at the ROCK beamline was employed:[35] By using the GUI, the data were merged to improve the signal to noise ratio after energy interpolation according to an energy grid specific to each edge. Normalization was performed by defining an absolute energy scale of the maximum of the first derivative of the metal reference foil to the tabulated one, *i.e.,* 20003.9 eV for Mo K- and 7709 eV for Co K-edge.

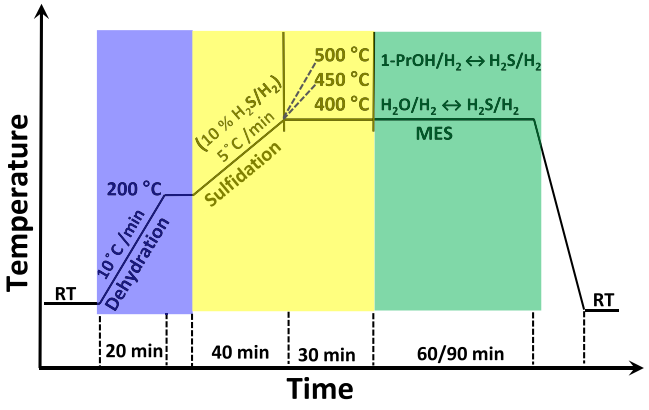

Figure 1. Schematic overview of steps performed during catalyst activation (dehydration and sulfidation) and MES experiments.

2.3. Modulation Excitation Spectroscopy (MES) and X-ray Absorption Spectroscopy (XAS) Data Analysis. One MES experiment consisted of 10−15 periods of 6 min each while recording XAS spectra with a frequency of 2 Hz, making a total of 7200−10,800 spectra during one run of 60/90 min. To deal with the large amount of data, MES analysis was performed using MatLab scripts where these normalized spectra were first averaged in 10 s intervals to obtain a set of 36 time-resolved spectra. This averaging enhanced the signal-to-noise ratio for detection of small changes during a 360 s period. These time-resolved spectra were transformed into phase-resolved spectra using eq 1, which demodulates the averaged time-resolved series of spectra $\mu(E, t)$[36,37] into a phase-resolved set $\mu(E, \Delta\phi)$ by probing with a sine function of period T = 360 s and phase shift $\Delta\phi$, $0° \leq \Delta\phi < 360°$. Thereby, periodic changes occurring at identical phase shifts during each period are added up, making them detectable.

$$\mu(E, \Delta\varphi) = \frac{2}{T}\int_0^T \mu(E, t)\sin\left(\frac{360°}{T}t + \Delta\varphi\right)\mathrm{d}t \quad (1)$$

The phase-resolved spectra were analyzed qualitatively and quantitatively by comparing them to difference spectra of pairs of compounds expected to result from the two alternating reaction conditions.

Extended X-ray absorption fine structure (EXAFS) spectra of the reference compounds MoO_3, MoO_2, MoS_2, Co_9S_8, Co_3S_4, CoO, $CoAl_2O_4$, Co_2O_3, Co_3O_4, CoAl-LDH, and $CoMoO_4$ were recorded for calibration and analysis purposes. Fourier transformation (FT) of the resulting spectrum from k-space to R-space and theoretical model fitting was performed using the software package IFEFFIT interfaces Athena and Artemis.[38] Model structures obtained from references, *i.e.,* sulfides and oxides of the corresponding metals, have been used to fit the experimental data in R-space for determining the structural parameters. These parameters include energy shift of the path (ΔE_0), change in the half path length (ΔR), amplitude reduction factor (S_0^2), number of identical paths (N), and relative mean-square displacement of the atoms included in path (Debye−Waller factor, σ^2). At the Mo K-edge, EXAFS spectra were fitted in the range of R = 1.0−4.0 Å and k = 2.1−12.4 $Å^{-1}$. The amplitude reduction factor (S_0^2), as determined from Mo foil, was fixed at 0.97, and one energy

https://doi.org/10.1021/acscatal.1c04767
ACS Catal. 2022, 12, 633−647

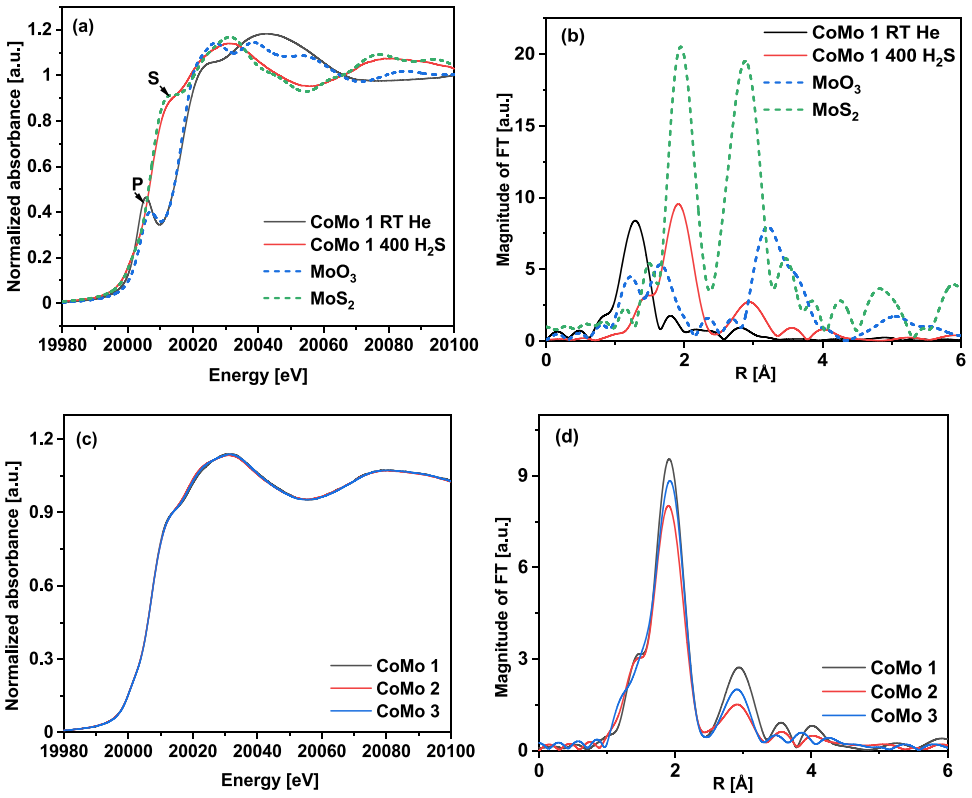

Figure 2. (a) Mo K-edge XANES spectra for the pre-calcined CoMo 1 catalyst at RT (black curve) and *in situ* sulfided catalyst at 400 °C (red curve) along with the MoO_3 (blue dashed curve) and MoS_2 reference spectra (green dashed curve) and (b) the corresponding Fourier transform spectra. (c) Mo K-XANES spectra for *in situ* sulfided CoMo catalysts with different metal loadings and (d) the corresponding Fourier transform spectra.

Table 2. Structural Parameters Obtained from EXAFS Analysis at the Mo K-Edge for the CoMo Catalysts with Different Metal Loadings[a]

	scattering paths and obtained fitting parameters									
sample	Mo-O1			Mo-S			Mo-Mo			
400 °C H_2S	R (Å)	CN	σ^2 (Å^2)	R (Å)	CN	σ^2 (Å^2)	R (Å)	CN	σ^2 (Å^2)	E_0, χ_ν^2
CoMo 1	1.63	0.20 ± 0.09	0.0038 ± 0.0014[b]	2.42	4.9 ± 0.3	0.0075 ± 0.0005	3.19	1.3 ± 0.1	0.0051 ± 0.0025[b]	3.1 ± 0.8 eV, 3
CoMo 2	1.60	0.23 ± 0.06	0.0038 ± 0.0014[b]	2.42	4.8 ± 0.2	0.0081 ± 0.0004	3.19	0.9 ± 0.1	0.0051 ± 0.0025[b]	3.4 ± 0.6 eV, 6
CoMo 3	1.60	0.20 ± 0.08	0.0038 ± 0.0014[b]	2.41	4.7 ± 0.3	0.0087 ± 0.0006	3.18	0.8 ± 0.1	0.0051 ± 0.0025[b]	2.9 ± 0.7 eV, 20

[a] S_0^2 is fixed to 0.97 as determined by Mo metal foil. [b] Fixed during the fitting.

shift parameter (E_0) was defined for all scattering paths. Scattering paths Mo-O, Mo-S, and Mo-Mo obtained from reference models were used and parameters N, ΔR, and σ^2 were fitted. σ^2 for the Mo-O bond has been fixed to the value as determined from the pre-calcined sample, and σ^2 for the Mo-Mo path has been fixed to the value as determined from MoS_2. At the Co K-edge, EXAFS spectra were fitted in the range of R = 1.0−4.0 Å and k = 2.8−11.5 Å^{-1}. The amplitude reduction factor (S_0^2), as determined from Co foil, was fixed at 0.83 and one energy shift parameter (E_0) was defined for all scattering paths. Scattering paths Co-S, Co-Co1, Co-Co2, Co-Al and Co-Mo obtained from reference models were used and parameters N, ΔR, and σ^2 were fitted.

3. RESULTS AND DISCUSSION

3.1. Effect of Metal Loading and Temperature on the Active Sites of CoMo Catalysts.

3.1.1. Active Phase of Mo after In Situ Sulfidation. Figure 2a shows the Mo K-edge X-ray absorption near edge structure (XANES) spectra of the CoMo 1 catalyst at room temperature under He (black curve) and after *in situ* sulfidation at 400 °C under H_2S (red curve) along with the reference spectra of MoO_3 (blue dashed curve) and MoS_2 (green dashed curve). The formation of the Mo(IV)S_2 phase was confirmed by the complete depletion of the pre-edge peak P, shifting of the edge toward lower energy, and appearance of the feature S at 20,012 eV, *i.e.*, characteristic features observed in the MoS_2 reference spectrum. In the corresponding Fourier transformed (FT) EXAFS spectra shown in Figure 2b, the first peak around 2 Å (not phase corrected) shows the presence of Mo-S backscattering similar

https://doi.org/10.1021/acscatal.1c04767
ACS Catal. 2022, 12, 633−647

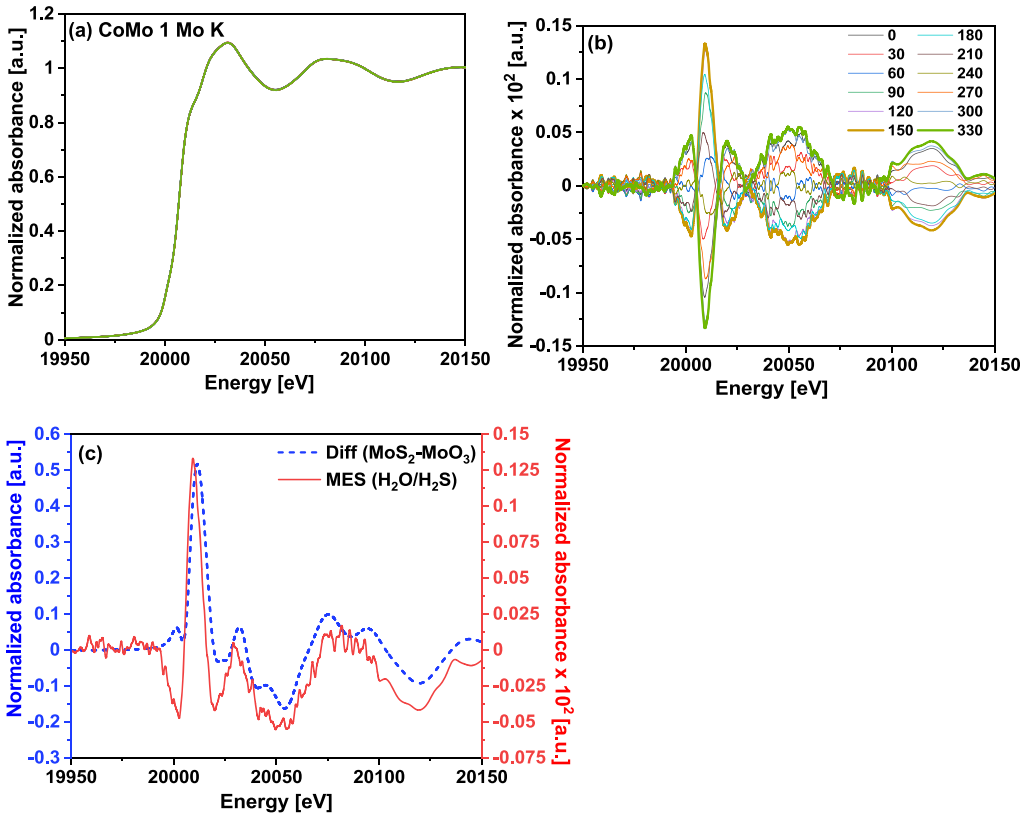

Figure 3. (a) Normalized, time-resolved Mo K-edge XANES consisting of a total of 36 spectra covering 10 s each for the CoMo 1 catalyst during 3% H_2O/H_2 (0−180 s) vs 500 ppm H_2S/H_2 (180−360 s) cycling and 10 period average. (b) Corresponding demodulated spectra at selected values of phase angle ($\Delta\phi$). (c) Comparison of the (MoS_2 − MoO_3) difference spectrum (blue dashed line) with the maximum amplitude signal obtained at $\Delta\phi$ = 150° after demodulation (red line) for the CoMo 1 catalyst.

to the reference MoS_2. The amplitude of this peak is almost half compared to that for bulk MoS_2, indicating a decrease in Mo-S coordination, *i.e.*, the presence of vacancies. The second peak, which corresponds to Mo-Mo backscattering, is observed with very low amplitude, indicating a smaller particle size than bulk MoS_2. However, the decrease in amplitude of the backscattering contributions in the FT EXAFS spectra is not only correlated to the coordination numbers but also to the structural as well as the thermal disorder. Hence, these changes need to be substantiated by EXAFS fitting. Figure 2c,d shows the Mo K-XANES and FT EXAFS spectra of the *in situ*-sulfided CoMo samples with different metal loadings, respectively. The XANES features indicate that the degree of sulfidation of the Mo sites in these samples was similar. In the FT EXAFS, comparatively high amplitude of the backscattering peaks is observed for CoMo 1 with the lowest metal loading. The structural parameters determined from fitting the EXAFS for these sulfide samples are given in Table 2, and corresponding fitting curves are given in the Supporting Information, Figure S1.

Mo-S backscattering was observed at ∼2.42 Å with CNs of 4.9, 4.8, and 4.7 for CoMo 1, CoMo 2, and CoMo 3, respectively. The Mo-S CN is 6 in the bulk phase, which indicates the presence of a MoS_2 phase with sulfur-deficient Mo sites in these catalysts as also reported by earlier studies.[5,10] A Mo-O contribution at 1.62−1.65 Å with a very low CN of ∼0.24 has been explained as interaction with the support with no actual bonding between Mo and O.[39] The Mo-Mo coordination at 3.18−3.19 Å is also in agreement with earlier reported values. However, the CN of Mo-Mo was found to be slightly higher, *i.e.*, 1.3 for CoMo 1 with the lowest metal loading. Thus, it can be concluded that the Mo sulfide phase obtained after *in situ* sulfidation at 400 °C was similar for the CoMo samples with different metal loadings and complete sulfidation of the Mo oxide phase was achieved in each case, *i.e.*, the bulk phase for MES was MoS_2 with sulfur-deficient Mo sites.

3.1.2. Dynamic Changes over Mo Sites during H_2O vs H_2S Cycling by MES-Coupled XAS. Figure 3a shows 36 time-resolved XANES spectra at Mo K-edge (covering 10 s each) obtained during 3% H_2O/H_2 (0−180 s) vs 500 ppm H_2S/H_2 (180−360 s) cycling from averaging 10 periods for the sample CoMo 1. In these spectra, no changes were observed in the intensity and shape of features, which indicates that during H_2O/H_2S cycling, the bulk sulfide phase of Mo remained intact, as expected.[14] However, the small atomic changes occurring at the edges during cycling conditions could be probed by demodulating the time-resolved spectra into phase-resolved spectra, as given in Figure 3b. For clarity, the demodulated spectra are shown only at selected values of phase shift ($\Delta\phi$). During the demodulation process, the contribution from static species was removed and averaging over 10 periods provided a high signal-to-noise ratio.

As shown in Figure 3c, the features of the demodulated spectrum with the highest amplitude (phase shift $\Delta\phi$ = 150°) matched remarkably well to the difference between the spectra of the MoS_2 and MoO_3 references. This agreement shows that S-O exchange took place on Mo sites during H_2O/H_2 and H_2S/H_2 cycling. However, the amplitude of the demodulated spectrum was more than two orders of magnitude (a factor of

https://doi.org/10.1021/acscatal.1c04767
ACS Catal. 2022, 12, 633−647

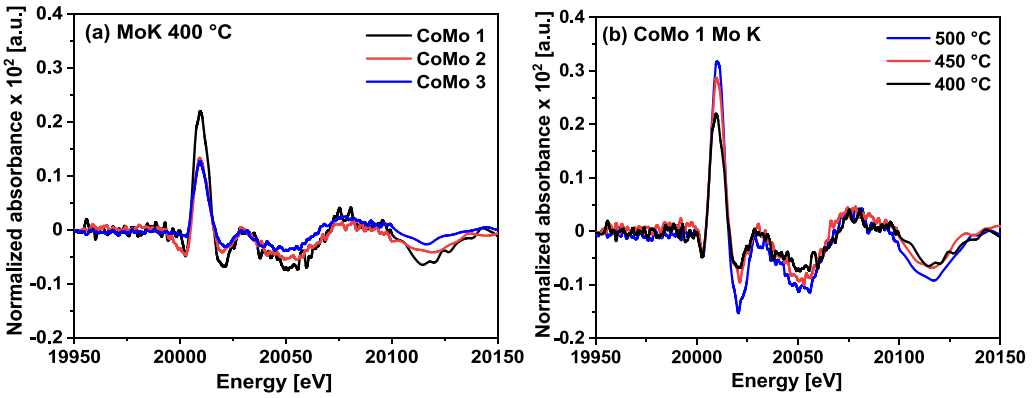

Figure 4. Comparison of the maximum amplitude signal obtained after demodulation at the Mo K-edge for the (a) CoMo catalysts with different metal loadings at 400 °C and the (b) CoMo 1 catalyst with cycling experiments performed at different temperatures. The black curve in both figures corresponds to the CoMo 1 catalyst at 400 °C, which can be taken as a reference to compare the effect of metal loading and temperature.

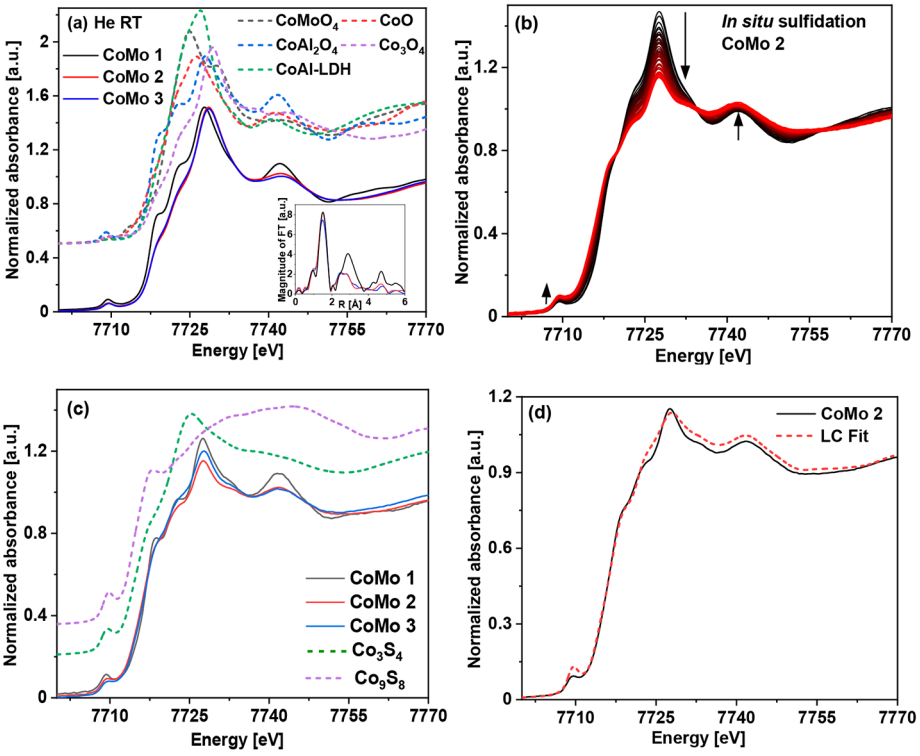

Figure 5. (a) Co K-edge XANES spectra for the calcined catalysts at RT along with the reference spectra and corresponding Fourier transformed EXAFS spectra (inset). (b) Normalized XANES spectra for the CoMo 2 catalyst during *in situ* sulfidation, (c) Co K-edge XANES spectra for the *in situ*-sulfided CoMo catalysts with different metal loadings along with the reference spectra of Co_3S_4 and Co_9S_8, (d) LCF analysis performed on the sulfided CoMo 2 catalyst.

400) smaller than the difference of the reference spectra, corresponding to a reversible oxidation−sulfidation process for approximately 2−3 Mo atoms for every thousand Mo atoms. Hence, minuscule changes occurring over the Mo sites, which were not possible to detect by conventional XAS, were successfully detected by coupling XAS with MES.

Similar cycling experiments were performed for the other two CoMo samples. The time-resolved spectra and corresponding demodulated spectra for CoMo 2 and CoMo 3 are given in the Supporting Information, Figure S2. Figure 4a compares the maximum amplitude obtained for the demodulated spectra at the Mo K-edge, where CoMo1 shows higher amplitude compared to CoMo 2 and CoMo 3, *i.e.*, lower CoMo loading resulted in a higher fraction of Mo sites undergoing S-O exchange. For CoMo 2 and CoMo 3, an almost equal amplitude of the demodulated spectra is obtained, which means a further increase in the metal loading will not affect the fraction of Mo sites prone to S-O exchange. As shown in Figure S2, the maximum amplitude of the demodulated spectra for CoMo 2 was observed at $\Delta\phi = 150°$, similar to that of CoMo1. In contrast, for CoMo 3, it was observed at $\Delta\phi = 120°$. This indicates that with higher metal loading, the changes occurred faster.

In another set of MES experiments, the cycling experiments were performed at higher temperatures with CoMo 1, *i.e.*, at 450 and 500 °C, to monitor the effect of temperature on the S-O exchange occurring at the Mo sites of the Co-promoted catalyst. The time-resolved spectra and corresponding

https://doi.org/10.1021/acscatal.1c04767
ACS Catal. 2022, 12, 633−647

Table 3. Structural Parameters Obtained from EXAFS Analysis at the Co K-Edge for the CoMo Catalysts with Different Metal Loadings[a]

sample	scattering paths and fitting parameters											
RT He	Co-O1			Co−Co1/Co2 (Co_3O_4[b])			Co-Al/Co3 ($CoAl_2O_4$[b])			Co-Mo ($CoMoO_4$[b])		
	R (Å)	CN	σ^2 (Å^2)	R (Å)	CN	σ^2 (Å^2)	R (Å)	CN	σ^2 (Å^2)	R (Å)	CN	σ^2 (Å^2)
CoMo 1	1.97	4.2 ± 0.6	0.0055 ± 0.0016	3.01/ 3.45	4[c]/ 2[c]	0.0130 ± 0.0050	3.45/ 3.60	6[c]/ 4[c]	0.0102 ± 0.0041	3.55	2[c]	0.0084 ± 0.0033
RT He	Co-O1			Co-Co1			Co-Mo					
	R (Å)	CN	σ^2 (Å^2)	R (Å)	CN	σ^2 (Å^2)	R (Å)	CN	σ^2 (Å^2)			
CoMo 2	1.93	4.4 ± 0.4	0.0056 ± 0.0010	3.00	4[c]	0.0126 ± 0.0016	3.33	2[c]	0.0110 ± 0.0020			
CoMo 3	1.93	4.4 ± 0.4	0.0053 ± 0.0008	3.00	4[f]	0.0132 ± 0.0015	3.31	2[c]	0.0122 ± 0.0021			
400 °C H_2S	Co-O1			Co-S			Co-Co					
	R (Å)	CN	σ^2 (Å^{2e})	R (Å)	CN	σ^2 (Å^2)	R (Å)	CN	σ^2 (Å^2)			
CoMo 2	1.87	1[c]	0.0049 ± 0.0027	2.22	2.6 ± 0.6	0.0074 ± 0.0020	3.00	2[c]	0.0131 ± 0.0024			

[a]S_0^2 is fixed to 0.83 as determined by Co metal foil. [b]Paths taken from Co reference model. [c]Fixed during the fitting.

demodulated spectra for CoMo 1 at 450 and 500 °C are given in the Supporting Information, Figure S3. Figure 4b shows that with increasing temperature, the maximum amplitude increased. Thus, at higher temperature an increased fraction of Mo sulfide sites was oxidized under the effect of H_2O. This likely reflects a change in equilibrium toward the oxides at increasing temperature. The maximum amplitude of demodulated spectra was observed at $\Delta\phi$ = 120° (Figure S3) when performing MES experiments at 450 and 500 °C, showing that at higher temperature, the S-O exchange takes place at a faster rate than MES at 400 °C ($\Delta\phi$ = 150°). The *Y*-axis of both Figure 4a,b are kept at same range in order to directly compare the effect of loading and temperature on S-O exchange for the Co-promoted MoS_2 catalyst. Based on MES-XAS analysis in the present study, the two factors were observed to act in the opposite direction, *i.e.*, an increase in metal loading stabilizes the catalyst against the unwanted S-O exchange, whereas an increase in temperature makes the catalyst more prone to such a process.

3.1.3. Active Phase of Co Sites after In Situ Sulfidation. Figure 5a shows the Co K-edge XANES spectra of the CoMo catalysts at room temperature under He along with the spectra of the Co references $CoAl_2O_4$, CoO, Co_3O_4, $CoMoO_4$, and CoAl-LDH. The initial oxidized phase of Co is found to be different in CoMo 1 compared to CoMo 2 and CoMo 3, probably due to the lower metal loading. In CoMo 1, the characteristic features of $CoAl_2O_4$ are prominent, thus indicating higher contribution from this phase. This has been confirmed by XANES linear combination fitting (LCF) (shown in Figure S4) where in CoMo 1, 65% $CoAl_2O_4$ was found to be present along with 17% CoAl-LDH and 18% Co_3O_4. On the other hand, CoMo 2 had 16% $CoAl_2O_4$ with 14% CoAl-LDH and 70% Co_3O_4, while CoMo 3 had 17% $CoAl_2O_4$ with 17% CoAl-LDH and 66% Co_3O_4. Thus, CoMo 2 and CoMo 3 had almost the same phase compositions. The hydrotalcite-like phase evolving from Co and Al (CoAl-LDH) must be present before calcination. During calcination, this CoAl-LDH phase decomposed into nano Co_3O_4 and $CoAl_2O_4$, but when the catalyst is exposed to air moisture, a part of decomposed LDH can be reformed.

The FT EXAFS spectra shown in the inset of Figure 5a also indicate a different coordination environment in CoMo 1 as compared to CoMo 2 and CoMo 3. From EXAFS fitting results, given in Table 3 and Supporting Information Figure S5, Co-Al backscattering was observed at 3.45 Å in CoMo 1 in the higher metal shells, along with Co−Co and Co-Mo. In the case of CoMo 2 and CoMo 3, only Co-Co and Co-Mo backscattering were observed. However, for all CoMo samples Co-O backscattering was observed at ∼1.93 Å with a CN slightly higher than 4, as expected for a mixture of cobalt species. The large values of the DW factor for metal−metal shells represent the higher disorder in the calcined CoMo samples due to the presence of mixed phases of $CoAl_2O_4$, CoAl-LDH, and Co_3O_4.

Normalized Co K-XANES spectra for the CoMo 2 during *in situ* sulfidation are given in Figure 5b. The intensity of pre-edge feature at ∼7710 eV increased, whereas the white line intensity decreased considerably, indicating sulfidation of Co oxide. For comparison, normalized XANES spectra for the CoMo catalysts after *in situ* sulfidation at 400 °C under H_2S are shown in Figure 5c. As expected, differences between the sulfide phases can be observed for the catalysts due to the presence of different oxide phases initially and the incomplete sulfidation of these oxide phases. For confirming the contribution of different phases present in the sulfided catalysts, LCF analysis using probable standards were performed. Figure 5d shows the LCF performed on CoMo 2 using the different reference spectra (*c.f.*, Table 4) where good agreement between the data and fit was observed. The corresponding LCF analysis performed on CoMo 1 and CoMo 3 is given in the Supporting Information, Figure S4.

Table 4. Linear Combination Fitting Results for the *In Situ* Sulfided CoMo Catalysts at 400 °C

	contribution obtained by LCF(%)			
sample	Co_3S_4	Co_9S_8	$CoAl_2O_4$	CoAl-LDH
CoMo 1	0	44.2	46.6	9.0
CoMo 2	25.8	44.2	25.6	4.4
CoMo 3	15.9	44.8	25.6	13.6

LCF results given in Table 4 confirmed that CoMo 1 (with lowest loading) was least sulfided with 44.2% contribution from Co_9S_8, due to the relatively larger amount of $CoAl_2O_4$, which does not sulfide. CoMo 2 had ∼70% contribution from Co sulfide species, whereas CoMo3 had ∼61% with major fraction coming from Co_9S_8 and minor fraction from Co_3S_4. For all three sulfided CoMo catalysts, contribution from the Co_9S_8 phase is almost similar (∼44%). Thus, partial sulfidation of Co species was observed since cobalt aluminate does not

https://doi.org/10.1021/acscatal.1c04767
ACS Catal. 2022, 12, 633−647

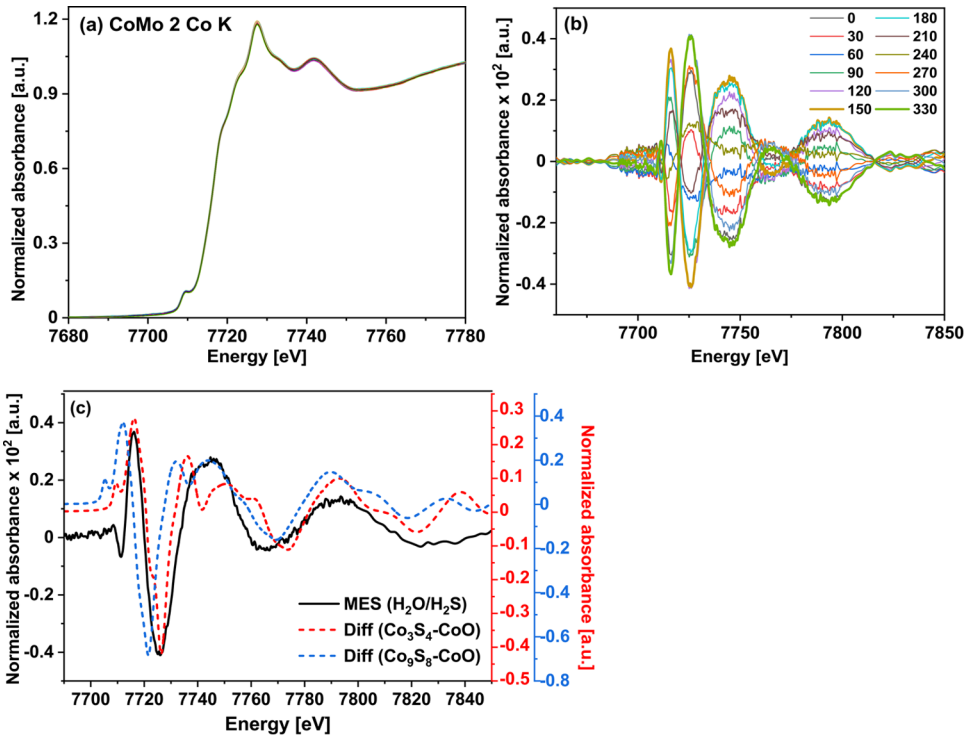

Figure 6. (a) Normalized, time-resolved Co K-edge XANES consisting of a total of 36 spectra covering 10 s each for the CoMo 2 catalyst during 3% H_2O/H_2 (0−180 s) vs 500 ppm H_2S/H_2 (180−360 s) cycling and 10 period average. (b) Corresponding demodulated spectra at selected phase angles ($\Delta\phi$). (c) Comparison of the (Co_3S_4 − CoO) and (Co_9S_8 − CoO) difference spectra (red and blue dashed lines) with the maximum amplitude signal obtained after demodulation (black line) for the catalyst.

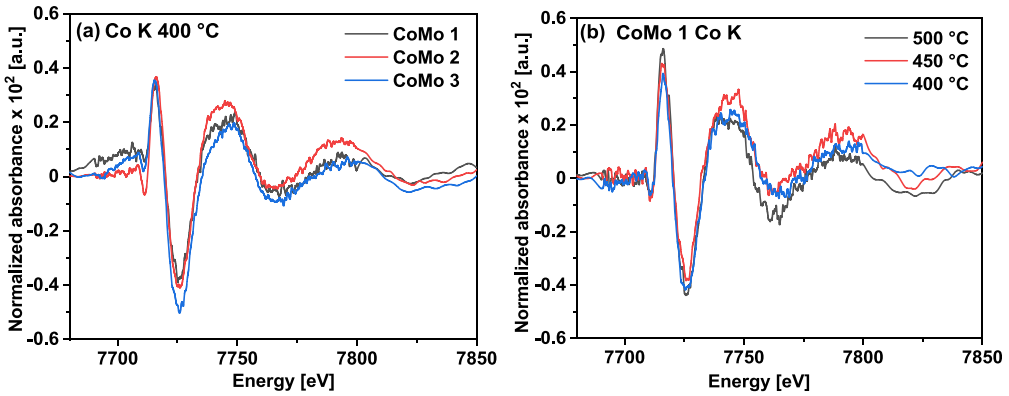

Figure 7. Comparison of the maximum amplitude signal obtained after demodulation at the Co K-edge for the (a) CoMo catalysts with different metal loadings and (b) the CoMo 1 catalyst with cycling experiments performed at different temperatures.

sulfide. It is to be mentioned here that the active sulfide phase for Co-promoted MoS_2 catalysts also consists of the CoMoS phase,[40,41] whose quantification requires rigorous data analysis,[16] which was not attempted here. The small contribution from CoAl-LDH shows the presence of this Co oxide species, which is in agreement with the results reported earlier.[16]

The EXAFS fitting for the sulfided CoMo 2 catalysts is given in the Supporting Information, Figure S5, and the fitting results for CoMo 2 are given in Table 3. The first shell had a contribution from Co-O with a CN of 1 (fixed) and Co-S with a CN of 2.6, confirming the presence of mixed phases. In the higher shells, Co-Co backscattering was observed at 3.00 Å. Fitting the EXAFS spectra of the other two sulfided CoMo catalysts did not give reasonable parameters, probably due to the higher presence of mixed Co oxide phases. Thus, the bulk phase before MES was a mixture of sulfide phases of Co and $CoAl_2O_4$. However, cobalt is expected to be stable as $CoAl_2O_4$ during the cycling and the advantage of MES is that this phase can be discriminated and only the active sulfide phase of Co is studied.

3.1.4. Dynamic Changes over Co Sites during H_2O vs H_2S Cycling by MES-Coupled XAS. Figure 6a shows time-resolved XANES spectra of the sulfided CoMo 2 catalyst at the Co K-edge during H_2O vs H_2S cycling obtained from averaging 10 periods. Again, no changes can be observed in the characteristic features. This shows that Co species did not undergo any major phase transition during cycling conditions as compared with the state obtained after sulfidation at 400 °C. The corresponding demodulated spectra of the CoMo 2 catalyst during H_2O vs H_2S cycling are shown in Figure 6b. Strong features can be observed here, which were undetectable in

https://doi.org/10.1021/acscatal.1c04767
ACS Catal. 2022, 12, 633−647

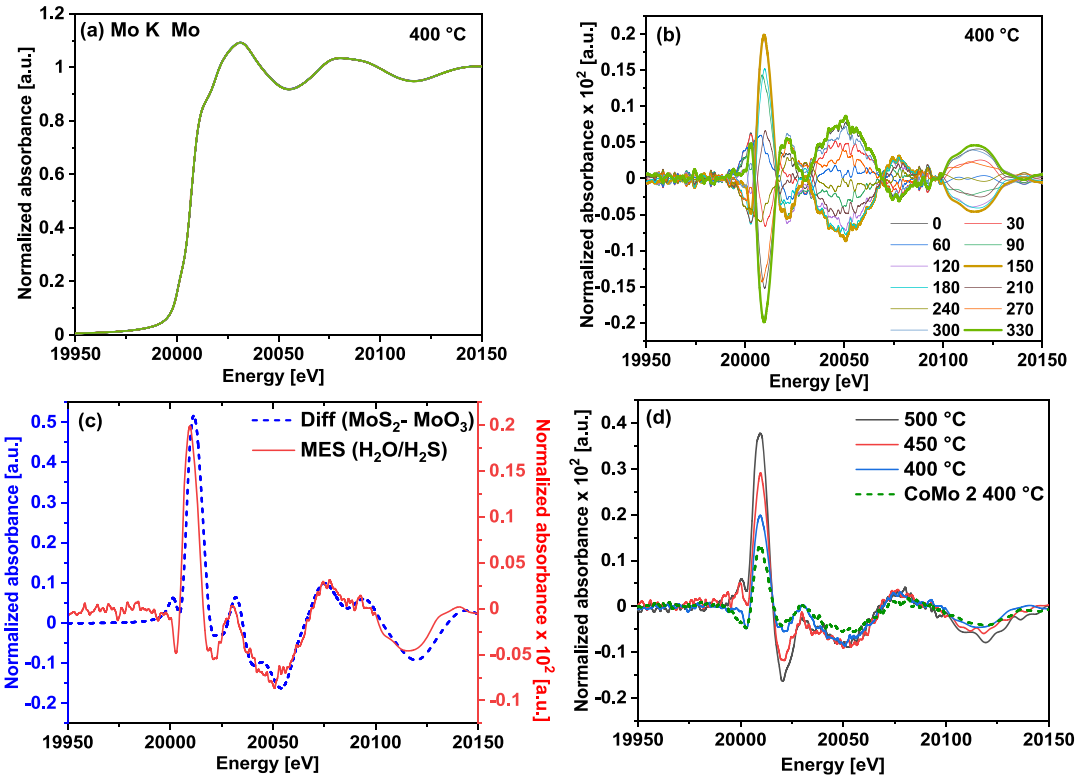

Figure 8. (a) Time-resolved spectra for the unpromoted Mo catalyst at the Mo K-edge during 3% H_2O/H_2 (0−180 s) vs 500 ppm H_2S/H_2 (180−360 s) cycling at 400 °C. (b) Corresponding demodulated spectra at selected values of the phase angle ($\Delta\phi$). (c) Comparison of the (MoS_2 − MoO_3) difference spectrum (blue dashed line) with the maximum amplitude signal obtained after demodulation (red line). (d) Comparison of the maximum amplitude signal obtained after demodulation at the Mo K-edge for the Mo catalyst at different temperatures and for CoMo 2 at 400 °C.

time-resolved spectra, indicating that minute changes do occur at Co sites. The maximum amplitude was observed at phase shift $\Delta\phi$ = 150°, which was also the case for MES-XAS at the Mo K-edge, indicating that the changes occur at a similar rate for both Co and Mo sites. These features can be resolved by comparing the demodulated spectrum with the maximum amplitude to the difference spectra of the references, *i.e.*, (Co_3S_4 − CoO) and (Co_9S_8 − CoO) as shown in Figure 6c.

A good agreement is observed between the demodulated spectrum obtained experimentally and difference spectra from references. Though the shapes look almost same for the two difference spectra, the (Co_9S_8 − CoO) spectrum is a bit shifted to lower energy and the (Co_3S_4 − CoO) fits better in the white line region. This demonstrates that some Co sulfide sites were oxidized and resulfided during H_2O/H_2 and H_2S/H_2 cycling, respectively. In addition, difference spectra of Co sulfide references with other Co oxide references, *i.e.*, Co_2O_3 and Co_3O_4 were also compared with the demodulated spectrum, but a satisfactory match was not obtained. This indicates that during cycling, the Co sulfide species reversibly transformed into Co^{2+} oxide species only.

In order to study the effect of metal loading on the reversible oxidation−sulfidation of Co sites, similar transient XAS experiments were performed on the other two catalysts, *i.e.*, CoMo 1 and CoMo 3. The time-resolved spectra and corresponding demodulated spectra at the Co K-edge for CoMo 1 and CoMo 3 are given in the Supporting Information, Figure S6. Figure 7a compares the maximum amplitude of the demodulated spectra obtained for CoMo 1, CoMo 2, and CoMo 3. A higher intensity of the feature at 7725 eV is observed in the case of CoMo 3, indicating an increase in the fraction of Co sites that underwent transformation during cycling with increasing metal loading. For CoMo 1, the maximum amplitude was observed at $\Delta\phi$ = 150° (Figure S6) similar to that of CoMo 2; however, for CoMo 3, it was observed at $\Delta\phi$ = 120°. This indicates that with higher metal loading, the changes occurred faster also at Co sites, like at Mo sites.

As mentioned earlier, the cycling experiments were performed for CoMo 1 at higher temperatures, i.e., 450 and 500 °C, to monitor the effect of temperature on the transitions occurring at the Mo sites as well as Co sites. The time-resolved spectra and corresponding demodulated spectra at Co K-edge for CoMo 1 at 450 and 500 °C are given in the Supporting Information, Figure S7. Figure 7b shows the comparison of the demodulated spectra at different temperatures. A small increase in the amplitude is observed with increasing temperature; however, this variation in the amplitude was of the order of the spectral noise. At 450 °C, the maximum amplitude was observed at $\Delta\phi$ = 120° (Figure S7), whereas at 500 °C, this value was observed to be 150°, the same as at 400 °C.

Thus, there is no clear sign that the phase changes occurring at Co sites during cycling were affected by increasing temperature. Hence, the Co sites showed a different behavior compared to the Mo sites where an influence of the temperature was found (Figure 4). Thus, Mo sites were comparatively more affected by the increase in temperature and metal loading than the Co sites, indicating the stable nature of Co sites under these cycling conditions. In a previous study[15] on these CoMo samples, by analyzing HAADF-STEM images of spent catalyst samples from 450 °C catalytic

https://doi.org/10.1021/acscatal.1c04767
ACS Catal. 2022, 12, 633−647

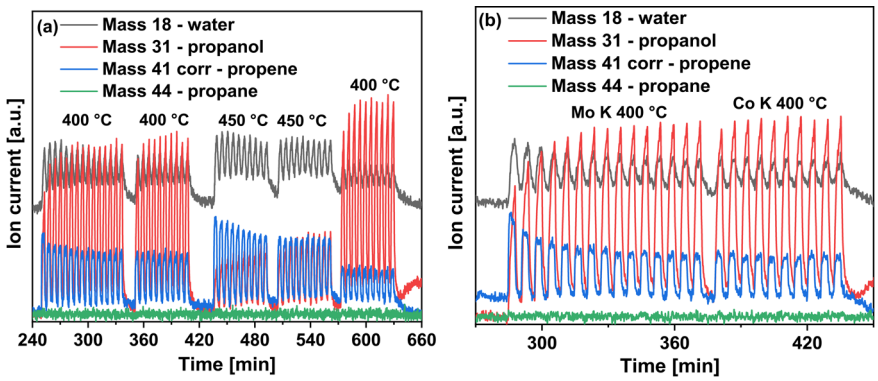

Figure 9. MS signal during 1-propanol/H_2−H_2S/H_2 cycling for (a) the Mo catalyst where a total of five MES experiments were performed at the Mo K-edge focusing the X-ray beam at the inlet and outlet positions of the quartz microreactor at 400 and 450 °C and (b) the CoMo 2 catalyst where two MES experiments were performed, one at the Mo K-edge and another at the Co K-edge, both focusing the X-ray beam at the inlet position of the microreactor at 400 °C. The MS signal encompasses the activity of the entire catalyst loaded in the microreactor.

hydropryolysis experiments, the mean slab length was found to be between 2.65 and 3.07 nm and the frequency of monolayer slabs was between 94 and 99%, indicating a similar degree of stacking. It was shown that cobalt, molybdenum, and sulfur were well-distributed on the alumina, indicating successful incorporation of the Co into the MoS_2 structure (CoMoS phase). The similar slab lengths, degree of stacking, and formation of the CoMoS phase showed that the catalysts were representative for comparing the effect of the CoMo loading.

Assuming the MoS_2 particles formed upon sulfidation, which are typically 3−4 nm slabs of 1−2 layers,[5,15] are the same for all CoMo catalysts and hence the ratio of surface to "bulk" Mo atoms should also be the same in this case. A similar size of these MoS_2 particles present in the CoMo catalysts can also be corroborated from the comparable CNs obtained from EXAFS fits (Table 2). Thus, a higher fraction of Mo sites undergoing S-O exchange for CoMo 1 (*c.f.*, Figure 4a) is related to the CoMo 1 catalyst having a larger fraction of $CoAl_2O_4$ than the other two catalysts. This Co will not be available for the promotion of the MoS_2 and hence protection from S-O exchange in the presence of H_2O.

3.2. Effect of Temperature and Promotion in the Demodulated Spectra of Unpromoted Mo Catalyst during H_2O/H_2-H_2S/H_2 Cycling. Figure 8a shows 36 time-resolved XANES spectra at the Mo K-edge (covering 10 s each) during 3% H_2O/H_2 (0−180 s) vs 500 ppm H_2S/H_2 (180−360 s) cycling at 400 °C obtained from averaging 10 periods for the sample Mo. No changes can be detected in these spectra, showing that the bulk phase for MES was MoS_2. This has been confirmed by comparison with the spectra of references and EXAFS fitting results given in the Supporting Information, Figure S8 and Table S1. Corresponding demodulated XANES spectra at 400 °C are shown in Figure 8b, where the expected features indicating minute changes occurring at Mo sites can be clearly observed. The features of the demodulated spectrum with the highest amplitude (phase shift $\Delta\phi$ = 150°) matched the difference spectrum of the MoS_2 and MoO_3 references, as shown in Figure 8c. This agreement shows that S-O exchange took place on Mo sites during H_2O/H_2 and H_2S/H_2 cycling.

To monitor the effect of temperature on the S-O exchange occurring at the Mo sites of the unpromoted catalyst, MES experiments were also performed at higher temperatures, 450 and 500 °C. The time-resolved spectra and corresponding demodulated spectra at the Mo K-edge for Mo at 450 and 500 °C are given in the Supporting Information, Figure S9. Figure 8d gives a comparison of the maximum amplitude for demodulated spectra obtained at the different temperatures for the unpromoted Mo catalyst. It can be seen that with increasing temperature, the maximum amplitude increased, *i.e.*, 0.0020 at 400 °C, 0.0029 at 450 °C, and 0.0038 at 500 °C. Thus, with an increase of 100 °C, the fraction of Mo sulfide sites undergoing S-O exchange almost doubled, indicating that the unpromoted catalyst will be more prone to such undesired changes at higher temperatures, probably due to the shift of the equilibrium toward the oxide. The maximum amplitude (Figure S9) was observed at $\Delta\phi$ = 120° in the case of MES experiments at 450 and 500 °C, showing a faster rate at higher temperature, similar to the nature of Mo sites observed in the case of CoMo 1. In Figure 8d, the maximum amplitude demodulated spectrum for the CoMo 2 catalyst at 400 °C (0.0013) is also plotted (dashed curve), which is lower than that of the Mo catalyst at 400 °C, indicating a positive effect of Co promotion. This is in agreement with our previous study, where a decrease in S−O exchange upon promotion has been discussed in detail for Co/Ni-promoted Mo catalysts.[14]

3.3. Comparing the Effect of the Oxygenate Reactant on Demodulated Spectra: H_2O/H_2-H_2S/H_2 vs 1-Propanol/H_2−H_2S/H_2 Cycling. As water is the product of HDO, it is also relevant to perform the MES experiments with an oxygenate reactant instead of water. In the present case, the experiments were limited to gas phase reactants and feeding by bubbling hydrogen through a reservoir of liquid at room temperature. Hence, 1-propanol was chosen as the reactant due to the similar vapor pressure and the same number of oxygen atoms per molecule as water. A primary alcohol is expected to react over the HDO catalysts, forming the corresponding alkene or alkane, here propene or propane, by dehydration and hydrogenation reactions, respectively. Hence, MS traces were measured during the cycling experiments with 1-propanol/H_2−H_2S/H_2.

The MS traces during 1-propanol/H_2−H_2S/H_2 cycling for the Mo catalyst at 400 and 450 °C and for the CoMo 2 catalyst at 400 °C are shown in Figure 9. Conversion of 1-propanol (m/z = 31) to propene (m/z = 41, corrected for the 1-propanol contribution to this mass) and water (m/z = 18) was observed, but propane (m/z = 44) was not detected. Hence, only dehydration and no hydrogenation took place. This is likely due to the low pressure of hydrogen, since the MES experiments were performed at close to atmospheric pressure.

https://doi.org/10.1021/acscatal.1c04767
ACS Catal. 2022, 12, 633−647

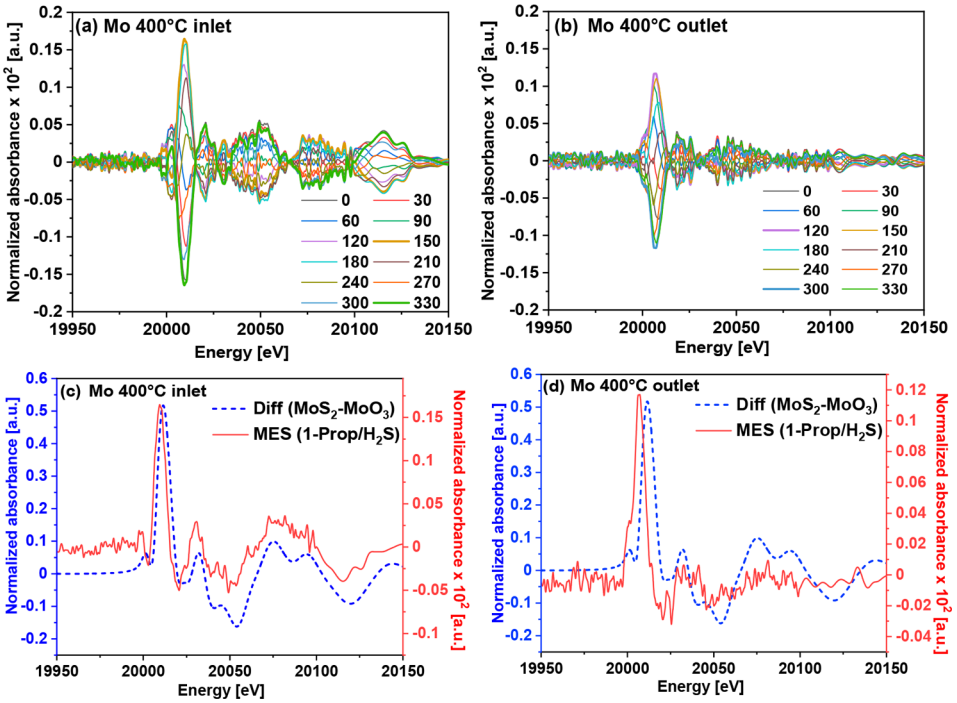

Figure 10. Demodulated spectra at selected values of phase angle ($\Delta\phi$) for the unpromoted Mo catalyst during 1-propanol/H_2 (0−180 s) vs 500 ppm H_2S/H_2 (180−360 s) cycling at the (a) inlet and (b) outlet of the quartz microreactor. Comparison of the (MoS_2 − MoO_3) difference spectrum (blue dashed line) with the maximum amplitude signal obtained after demodulation (red line) for the catalyst at the (c) inlet and (d) outlet of the microreactor.

From Figure 9, a deactivation of the catalyst was observed during the first cycles at each temperature as the propene and water signal decreased in maximum intensity (amplitude of the peaks in the 1-propanol/H_2 cycle) and the 1-propanol signal increased in maximum intensity with each period. After about 5−6 periods for the Mo catalyst and 7−8 periods for the CoMo 2, the peak intensity became more or less constant. With the help of the focused beam (0.5 mm (H) × 0.3 mm (V)) at the ROCK beamline, the spectra were measured alternately at the inlet as well as at the outlet position of the quartz microreactor to compare the state of the catalyst as function of the reactant conversion over the catalyst bed. A higher concentration of the reactant 1-propanol was present at the inlet, while a higher concentration of the products propene and water was present at the outlet due to conversion of 1-propanol.

Demodulated XANES spectra of the unpromoted Mo catalyst at the Mo K-edge during 1-propanol vs H_2S cycling at 400 °C are shown in Figure 10a,b, recorded at the inlet and outlet of the quartz microreactor, respectively. Corresponding time-resolved spectra are given in the Supporting Information, Figure S10, where no changes were observed, showing that the bulk phase for MES was MoS_2. The features observed at the inlet of the reactor are stronger and better resolved compared to those observed at the outlet. This could be due to interaction of the catalyst with the formed propene. Figure 10c,d gives the comparison of the features of the demodulated spectrum with the maximum amplitude observed at $\Delta\phi$ = 150° for the inlet and at $\Delta\phi$ = 120° for the outlet, respectively, together with the difference spectrum of the MoS_2 and MoO_3 references. At the inlet, good agreement between the two spectra shows that S-O exchange also occurred on Mo sites during 1-propanol/H_2 and H_2S/H_2 cycling. For the outlet, though the demodulated spectrum features are less resolved, they still show similarity with MoS_2-MoO_3 indicating the S-O exchange, as expected for water and 1-propanol interacting with the catalyst. Also, as observed from values of $\Delta\phi$ for the maximum amplitude, the changes at the outlet occur slightly faster. The demodulated spectra observed in this case showed some deviation from the expected behavior as some of the spectra do not have zero crossing on the Y-axis at the same energy, *i.e.*, no clear isosbestic point can be observed. This can be attributed to different reasons, e.g., that there are more than two species or that different parts of the sample have different reaction rates. The observed deviation is higher at the outlet than at the inlet. As mentioned above, a higher concentration of the products (propene and water) is present at the outlet, which may cause multiple-step transition or different reaction rates leading to dampening of features generally observed in the presence of two different phases.

The cycling experiments with 1-propanol were also performed at 450 °C (both inlet and outlet positions), and results are given in the Supporting Information, Figure S10. As expected, at 450 °C, a comparatively high amplitude of the demodulated spectra, *i.e.*, 0.0020 vs 0.0016 at 400 °C, indicates that with higher temperature, the amount of S-O exchange at Mo sites increased during 1-propanol vs H_2S cycling, like for H_2O vs H_2S cycling. At 450 °C the maximum amplitude was observed at $\Delta\phi$ = 150° (Figure S10) for both the inlet and outlet positions. From the MS traces (Figure 9), it was also observed that the conversion of 1-propanol to propene and water increased significantly, as expected, and the catalyst deactivated further during the first 8−9 cycles at 450 °C.

Similarly, MES experiments were performed with the CoMo 2 catalyst when cycling 1-propanol vs H_2S at the inlet position of the quartz microreactor. The maximum amplitude

https://doi.org/10.1021/acscatal.1c04767
ACS Catal. 2022, 12, 633−647

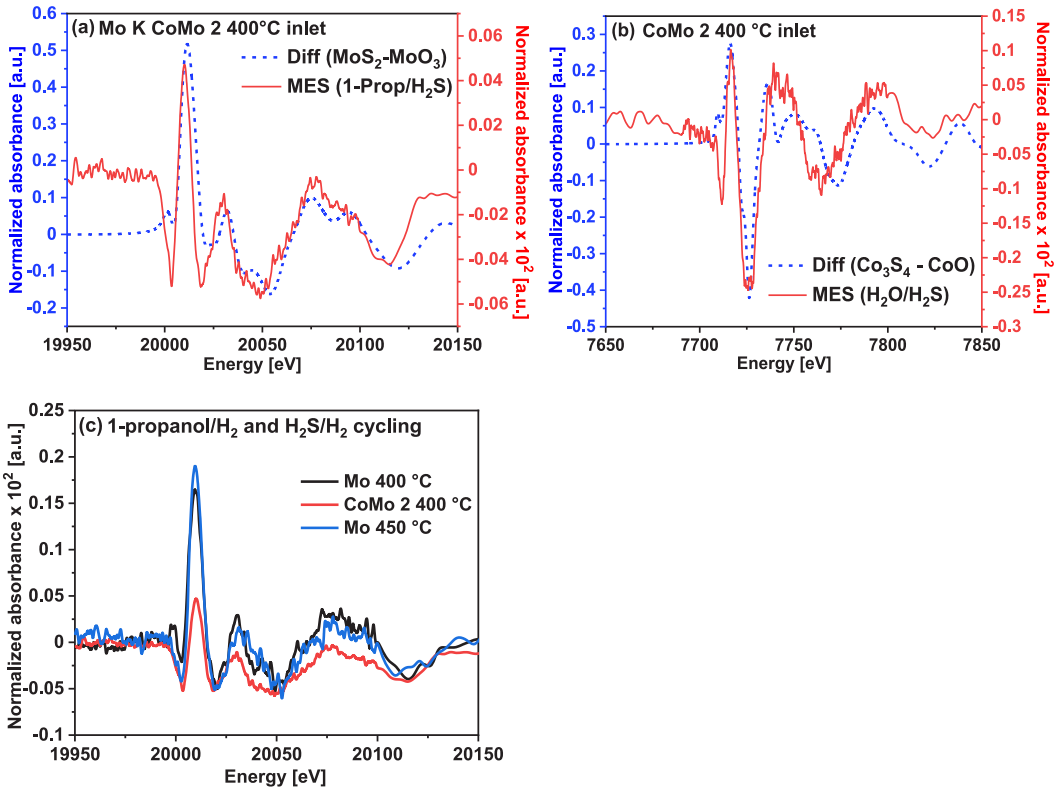

Figure 11. Demodulated spectra for CoMo 2 during 1-propanol/H_2 and H_2S/H_2 cycling for MES experiments performed at the inlet position of the quartz microreactor (a) comparison of the (MoS_2 − MoO_3) difference spectrum with the maximum amplitude signal obtained after demodulation at the Mo K-edge and (b) comparison of the (Co_3S_4 − CoO) difference spectrum with the maximum amplitude signal obtained after demodulation at the Co K-edge. (c) Comparison of demodulated maximum amplitude at the Mo K-edge for the Mo catalyst at 400 and 450 °C and for CoMo 2 catalyst at 400 °C, all measured at the inlet position.

demodulated spectra along with the difference spectra of references at the Mo K-edge and Co K-edge are shown in Figure 11a,b, respectively. Corresponding time-resolved spectra and demodulated spectra are given in the Supporting Information, Figure S11. The changes observed at the Mo as well as Co sites during 1-propanol vs H_2S cycling were similar to those observed for this catalyst during H_2O vs H_2S cycling, *i.e.*, at Mo sites, S-O exchange was observed, and at Co sites, oxidation of the sulfide phase was observed. The maximum amplitude of the demodulated spectra was observed at $\Delta\phi$ = 0° at both the Mo and Co K-edges (Figure S11), indicating that maximum changes occurred initially. In the case of CoMo 2, the amplitude of the demodulated spectrum at the Mo K-edge was observed to be quite low (0.0005) as compared to that of the unpromoted Mo sample (0.0016) as shown in Figure 11c. Thus, in the case of propanol, there was an almost 70% decrease in the amplitude due to Co promotion, which is almost double as compared to that in the case of water where a 35% decrease in the amplitude was observed (*c.f.*, Figure 8d). This indicates that promotion with Co makes the catalyst comparatively more stable toward S-O exchange for 1-propanol than H_2O. In general, for the Mo and CoMo samples, similar trends were observed with H_2O and 1-propanol cycling, *i.e.*, high temperature enhances S-O exchange and promotion with Co lowers this effect.

Figure 12 gives the comparison of the maximum amplitude of the demodulated spectra obtained from the two different cycling experiments, H_2O vs H_2S and 1-propanol vs H_2S, at similar temperatures. A higher amplitude was observed with H_2O for both the Mo and the CoMo 2 catalysts. Thus, it can be concluded that H_2O is more effective for S-O exchange compared to 1-propanol. For the CoMo 2 catalyst, the difference between the amplitude of the demodulated spectra under the influence of two oxygenate reactants was very pronounced at both Mo and Co sites, which indicates that promotion with Co made the catalyst more stable against such processes when induced by a primary alcohol, *i.e.*, 1-propanol.

4. CONCLUSIONS

Modulation excitation spectroscopy coupled with time-resolved X-ray absorption spectroscopy can provide valuable insight and complement to surface science studies by unraveling the minute levels of reversible S-O exchange at the active sites of Co promoted and unpromoted MoS_2 hydrotreating catalysts. Due to its more selective and higher sensitive nature compared to conventional XAS, MES coupled XAS showed that the degree of S-O exchange was affected by the metal loading, promotion, temperature, and oxygenate reactant. For CoMo catalysts, increasing the metal loading at 400 °C stabilized the catalyst against the undesired S-O exchange at Mo sites whereas increasing the temperature made the catalyst more prone to such processes. Transient XAS could successfully detect the reversible oxidation/sulfidation occurring over sulfided Co sites, even in the presence of multiple phases. For the unpromoted Mo catalyst, with an increase of 100 °C (from 400 to 500 °C), the fraction of Mo sulfide sites undergoing S-O exchange almost doubled, substantiating the reactive nature of Mo sites. For both CoMo and Mo catalysts, a comparison of cycling experiments using 1-propanol vs H_2S with H_2O vs H_2S showed that H_2O

https://doi.org/10.1021/acscatal.1c04767
ACS Catal. 2022, 12, 633−647

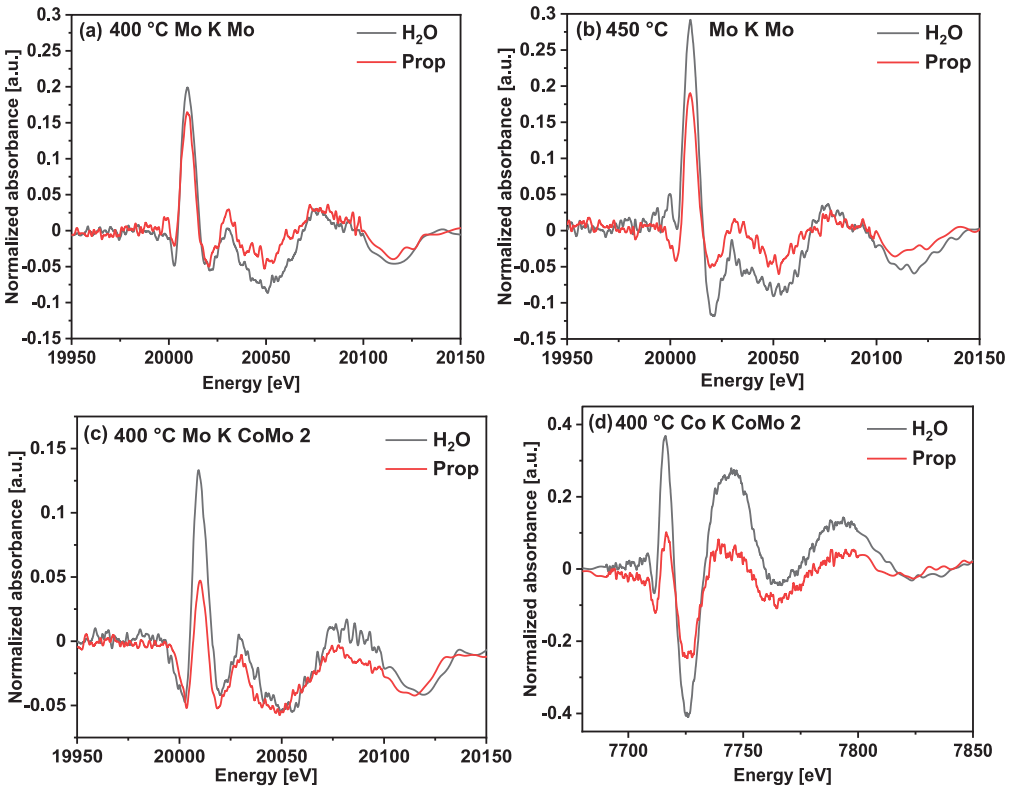

Figure 12. Comparison of the maximum amplitude of the demodulated spectra obtained from the two different cycling experiments H_2O vs H_2S and 1-propanol vs H_2S (inlet position of the quartz microreactor) at the Mo K-edge for (a) Mo at 400 °C, (b) Mo at 450 °C, (c) CoMo 2 at 400 °C, and (d) at the Co K-edge for CoMo 2 at 400 °C.

was more effective for S-O exchange than 1-propanol. For the CoMo catalyst, the difference was more pronounced at both Mo and Co sites under 1-propanol cycling as compared to H_2O cycling, which indicated that promotion with Co makes the catalyst more stable against such processes.

Thus, it has been shown that MES coupled with suitable time-resolved spectroscopic measurements can not only resolve the changes taking place on catalyst surfaces but can also evaluate the comparative degree of changes due to the variation in reaction conditions, e.g., temperature and sample composition, *i.e.*, metal loadings. These parameters play important roles in defining the activity and stability of the catalytic system, and hence, such sensitive measurements will be helpful in general to examine catalysts under *operando* conditions for characterization of the active site on the atomic scale.

■ ASSOCIATED CONTENT

Supporting Information

The Supporting Information is available free of charge at https://pubs.acs.org/doi/10.1021/acscatal.1c04767.

Additional time-resolved and demodulated XAS data at Mo K- and Co K-edge for CoMo (different metal loadings)/Mo catalysts at different temperatures during H_2O vs H_2S cycling; EXAFS fitting results for calcined and in situ sulfided catalysts at Mo K- and Co K-edge for CoMo/Mo catalysts; LCF results for calcined and *in situ* sulfided CoMo catalysts at Co K-edge; additional time-resolved and demodulated XAS data at Mo K- and Co K-edges for Mo/CoMo 2 catalysts at different temperatures during 1-propanol vs H_2S cycling at the inlet and outlet positions of the quartz microreactor (PDF)

■ AUTHOR INFORMATION

Corresponding Authors

Abhijeet Gaur − *Institute of Catalysis Research and Technology, Karlsruhe Institute of Technology (KIT), Eggenstein-Leopoldshafen D-76344, Germany; Institute for Chemical Technology and Polymer Chemistry, Karlsruhe Institute of Technology (KIT), Karlsruhe D-76131, Germany;* orcid.org/0000-0001-5328-9280; Email: abhijeet.gaur@kit.edu, abhijeetgaur9@gmail.com

Martin Høj − *Department of Chemical and Biochemical Engineering, Technical University of Denmark (DTU), Kgs. Lyngby DK-2800, Denmark;* orcid.org/0000-0002-8482-3359; Email: mh@kt.dtu.dk

Authors

Matthias Stehle − *Institute for Chemical Technology and Polymer Chemistry, Karlsruhe Institute of Technology (KIT), Karlsruhe D-76131, Germany;* orcid.org/0000-0002-7382-5666

Marc-André Serrer − *Institute of Catalysis Research and Technology, Karlsruhe Institute of Technology (KIT), Eggenstein-Leopoldshafen D-76344, Germany; Institute for Chemical Technology and Polymer Chemistry, Karlsruhe Institute of Technology (KIT), Karlsruhe D-76131, Germany*

Magnus Zingler Stummann − *Department of Chemical and Biochemical Engineering, Technical University of Denmark (DTU), Kgs. Lyngby DK-2800, Denmark;* orcid.org/0000-0001-6319-4429

https://doi.org/10.1021/acscatal.1c04767
ACS Catal. 2022, 12, 633−647

Camille La Fontaine − *SOLEIL Synchrotron, UR1-CNRS, L'Orme des Merisiers, BP48, Gif-sur Yvette F-91192, France*
Valérie Briois − *SOLEIL Synchrotron, UR1-CNRS, L'Orme des Merisiers, BP48, Gif-sur Yvette F-91192, France*
Jan-Dierk Grunwaldt − *Institute of Catalysis Research and Technology, Karlsruhe Institute of Technology (KIT), Eggenstein-Leopoldshafen D-76344, Germany; Institute for Chemical Technology and Polymer Chemistry, Karlsruhe Institute of Technology (KIT), Karlsruhe D-76131, Germany;* orcid.org/0000-0003-3606-0956

Complete contact information is available at: https://pubs.acs.org/10.1021/acscatal.1c04767

Notes

The authors declare no competing financial interest.

■ ACKNOWLEDGMENTS

The work at the ROCK beamline was supported by a public grant overseen by the French National Research Agency (ANR) as part of "Investissements d'Avenir" program (reference: ANR-10-EQPX-45). M.H. thanks DanScatt for funding travels to the SOLEIL synchrotron. We thank HGF for support in the programs "storage and crosslinked infrastructures" (SCI), "science and technology of nanosystems" (STN) and "Materials and Technologies for the Energy Transition" (MTET). We also thank KIT's synchrotron radiation source (operated by KIT-IBPT) for *ex situ* XAS measurements conducted at the CAT-ACT beamline.

■ REFERENCES

(1) Topsøe, H.; Clausen, B. S.; Massoth, F. E., Hydrotreating Catalysis. In *Catalysis: Science and Technology*, Anderson, J. R.; Boudart, M., Eds. Springer Berlin Heidelberg: Berlin, Heidelberg, 1996; pp. 1−269.
(2) Wang, H.; Male, J.; Wang, Y. Recent Advances in Hydrotreating of Pyrolysis Bio-Oil and Its Oxygen-Containing Model Compounds. *ACS Catal.* **2013**, *3*, 1047−1070.
(3) Badawi, M.; Paul, J.-F.; Cristol, S.; Payen, E. Guaiacol derivatives and inhibiting species adsorption over MoS_2 and CoMoS catalysts under HDO conditions: A DFT study. *Catal. Commun.* **2011**, *12*, 901−905.
(4) Bui, V. N.; Laurenti, D.; Afanasiev, P.; Geantet, C. Hydrodeoxygenation of guaiacol with CoMo catalysts. Part I: Promoting effect of cobalt on HDO selectivity and activity. *Appl. Catal. B* **2011**, *101*, 239−245.
(5) Dabros, T. M. H.; Gaur, A.; Pintos, D. G.; Sprenger, P.; Høj, M.; Hansen, T. W.; Studt, F.; Gabrielsen, J.; Grunwaldt, J.-D.; Jensen, A. D. Influence of H_2O and H_2S on the composition, activity, and stability of sulfided Mo, CoMo, and NiMo supported on $MgAl_2O_4$ for hydrodeoxygenation of ethylene glycol. *Appl. Catal. A* **2018**, *551*, 106−121.
(6) Furimsky, E. Catalytic hydrodeoxygenation. *Appl. Catal. A* **2000**, *199*, 147−190.
(7) Mortensen, P. M.; Grunwaldt, J.-D.; Jensen, P. A.; Knudsen, K. G.; Jensen, A. D. A review of catalytic upgrading of bio-oil to engine fuels. *Appl. Catal. A* **2011**, *407*, 1−19.
(8) Wang, Y.; Lin, H.; Zheng, Y. Hydrotreatment of lignocellulosic biomass derived oil using a sulfided NiMo/γ-Al_2O_3 catalyst. *Catal. Sci. Technol.* **2014**, *4*, 109−119.
(9) Kotrba, R. Where Will All the Feedstock Come From? *Biodiesel Magazine* **2019**, 2516631.
(10) Lauritsen, J. V.; Besenbacher, F. Atom-resolved scanning tunneling microscopy investigations of molecular adsorption on MoS_2 and CoMoS hydrodesulfurization catalysts. *J. Catal.* **2015**, *328*, 49−58.
(11) Ryymin, E.-M.; Honkela, M. L.; Viljava, T.-R.; Krause, A. O. I. Competitive reactions and mechanisms in the simultaneous HDO of phenol and methyl heptanoate over sulphided NiMo/γ-Al_2O_3. *Appl. Catal. A* **2010**, *389*, 114−121.
(12) Bollinger, M. V.; Jacobsen, K. W.; Nørskov, J. K. Atomic and electronic structure of MoS_2 nanoparticles. *Phys. Rev. B* **2003**, *67*, No. 085410.
(13) Bollinger, M. V.; Lauritsen, J. V.; Jacobsen, K. W.; Nørskov, J. K.; Helveg, S.; Besenbacher, F. One-Dimensional Metallic Edge States in MoS_2. *Phys. Rev. Lett.* **2001**, *87*, 196803.
(14) Gaur, A.; Hartmann Dabros, T. M.; Høj, M.; Boubnov, A.; Prüssmann, T.; Jelic, J.; Studt, F.; Jensen, A. D.; Grunwaldt, J.-D. Probing the Active Sites of MoS_2 Based Hydrotreating Catalysts Using Modulation Excitation Spectroscopy. *ACS Catal.* **2019**, *9*, 2568−2579.
(15) Stummann, M. Z.; Elevera, E.; Hansen, A. B.; Hansen, L. P.; Beato, P.; Davidsen, B.; Wiwel, P.; Gabrielsen, J.; Jensen, P. A.; Jensen, A. D.; Høj, M. Catalytic hydropyrolysis of biomass using supported CoMo catalysts − Effect of metal loading and support acidity. *Fuel* **2020**, *264*, 116807.
(16) Plais, L.; Lancelot, C.; Lamonier, C.; Payen, E.; Briois, V. First in situ temperature quantification of CoMoS species upon gas sulfidation enabled by new insight on cobalt sulfide formation. *Catal. Today* **2021**, *377*, 114−126.
(17) Grunwaldt, J.-D.; Caravati, M.; Hannemann, S.; Baiker, A. X-ray absorption spectroscopy under reaction conditions: suitability of different reaction cells for combined catalyst characterization and time-resolved studies. *Phys. Chem. Chem. Phys.* **2004**, *6*, 3037−3047.
(18) Grunwaldt, J.-D.; Wagner, J. B.; Dunin-Borkowski, R. E. Imaging Catalysts at Work: A Hierarchical Approach from the Macro- to the Meso- and Nano-scale. *ChemCatChem* **2013**, *5*, 62−80.
(19) Müller, P.; Hermans, I. Applications of Modulation Excitation Spectroscopy in Heterogeneous Catalysis. *Ind. Eng. Chem. Res.* **2017**, *56*, 1123−1136.
(20) Srinivasan, P. D.; Patil, B. S.; Zhu, H.; Bravo-Suárez, J. J. Application of modulation excitation-phase sensitive detection-DRIFTS for in situ/operando characterization of heterogeneous catalysts. *React. Chem. Eng.* **2019**, *4*, 862−883.
(21) König, C. F. J.; Schildhauer, T. J.; Nachtegaal, M. Methane synthesis and sulfur removal over a Ru catalyst probed in situ with high sensitivity X-ray absorption spectroscopy. *J. Catal.* **2013**, *305*, 92−100.
(22) König, C. F. J.; van Bokhoven, J. A.; Schildhauer, T. J.; Nachtegaal, M. Quantitative Analysis of Modulated Excitation X-ray Absorption Spectra: Enhanced Precision of EXAFS Fitting. *J. Phys. Chem. C* **2012**, *116*, 19857−19866.
(23) Lu, Y.; Keav, S.; Marchionni, V.; Chiarello, G. L.; Pappacena, A.; Di Michiel, M.; Newton, M. A.; Weidenkaff, A.; Ferri, D. Ageing induced improvement of methane oxidation activity of Pd/$YFeO_3$. *Catal. Sci. Technol.* **2014**, *4*, 2919−2931.
(24) Urakawa, A.; Van Beek, W.; Monrabal-Capilla, M.; Galán-Mascarós, J. R.; Palin, L.; Milanesio, M. Combined, Modulation Enhanced X-ray Powder Diffraction and Raman Spectroscopic Study of Structural Transitions in the Spin Crossover Material [Fe(Htrz)$_2$(trz)](BF$_4$). *J. Phys. Chem. C* **2011**, *115*, 1323−1329.
(25) Chiarello, G. L.; Ferri, D. Modulated excitation extended X-ray absorption fine structure spectroscopy. *Phys. Chem. Chem. Phys.* **2015**, *17*, 10579−10591.
(26) Ferri, D.; Newton, M. A.; Nachtegaal, M. Modulation Excitation X-Ray Absorption Spectroscopy to Probe Surface Species on Heterogeneous Catalysts. *Top. Catal.* **2011**, *54*, 1070.
(27) Stötzel, J.; Lützenkirchen-Hecht, D.; Frahm, R.; Grunwaldt, J.-D. Improving the sensitivity of QEXAFS using modulation excitation spectroscopy. *J. Phys.: Conf. Ser.* **2013**, *430*, No. 012126.
(28) Serrer, M.-A.; Gaur, A.; Jelic, J.; Weber, S.; Fritsch, C.; Clark, A. H.; Saraçi, E.; Studt, F.; Grunwaldt, J.-D. Structural dynamics in Ni−Fe catalysts during CO_2 methanation − role of iron oxide clusters. *Catal. Sci. Technol.* **2020**, *10*, 7542−7554.

(29) Czioska, S.; Boubnov, A.; Escalera-López, D.; Geppert, J.; Zagalskaya, A.; Röse, P.; Saraçi, E.; Alexandrov, V.; Krewer, U.; Cherevko, S.; Grunwaldt, J.-D. Increased Ir−Ir Interaction in Iridium Oxide during the Oxygen Evolution Reaction at High Potentials Probed by Operando Spectroscopy. *ACS Catal.* **2021**, 10043−10057.
(30) Frahm, R. Quick scanning exafs: First experiments. *Nucl. Instrum. Methods Phys. Res. A* **1988**, *270*, 578−581.
(31) Briois, V.; La Fontaine, C.; Belin, S.; Barthe, L.; Moreno, T.; Pinty, V.; Carcy, A.; Girardot, R.; Fonda, E. ROCK: the new Quick-EXAFS beamline at SOLEIL. *J. Phys.: Conf. Ser.* **2016**, *712*, No. 012149.
(32) Frahm, R. New method for time dependent x-ray absorption studies. *Rev. Sci. Instrum.* **1989**, *60*, 2515−2518.
(33) Fonda, E.; Rochet, A.; Ribbens, M.; Barthe, L.; Belin, S.; Briois, V. The SAMBA quick-EXAFS monochromator: XAS with edge jumping. *J. Synchrotron Radiat.* **2012**, *19*, 417−424.
(34) La Fontaine, C.; Belin, S.; Barthe, L.; Roudenko, O.; Briois, V. ROCK: A Beamline Tailored for Catalysis and Energy-Related Materials from ms Time Resolution to μm Spatial Resolution. *Synchrotron Radiat. News* **2020**, *33*, 20−25.
(35) Lesage, C.; Devers, E.; Legens, C.; Fernandes, G.; Roudenko, O.; Briois, V. High pressure cell for edge jumping X-ray absorption spectroscopy: Applications to industrial liquid sulfidation of hydro-treatment catalysts. *Catal. Today* **2019**, *336*, 63−73.
(36) Baurecht, D.; Fringeli, U. P. Quantitative modulated excitation Fourier transform infrared spectroscopy. *Rev. Sci. Instrum.* **2001**, *72*, 3782−3792.
(37) Urakawa, A.; Bürgi, T.; Baiker, A. Sensitivity enhancement and dynamic behavior analysis by modulation excitation spectroscopy: Principle and application in heterogeneous catalysis. *Chem. Eng. Sci.* **2008**, *63*, 4902−4909.
(38) Ravel, B.; Newville, M. ATHENA, ARTEMIS, HEPHAESTUS: data analysis for X-ray absorption spectroscopy using IFEFFIT. *J. Synchrotron Radiat.* **2005**, *12*, 537−541.
(39) Rochet, A.; Baubet, B.; Moizan, V.; Pichon, C.; Briois, V. Co-K and Mo-K edges Quick-XAS study of the sulphidation properties of Mo/Al_2O_3 and $CoMo/Al_2O_3$ catalysts. *C. R. Chim.* **2016**, *19*, 1337−1351.
(40) Gandubert, A. D.; Krebs, E.; Legens, C.; Costa, D.; Guillaume, D.; Raybaud, P. Optimal promoter edge decoration of CoMoS catalysts: A combined theoretical and experimental study. *Catal. Today* **2008**, *130*, 149−159.
(41) van Haandel, L.; Bremmer, G. M.; Hensen, E. J. M.; Weber, T. Influence of sulfiding agent and pressure on structure and performance of $CoMo/Al_2O_3$ hydrodesulfurization catalysts. *J. Catal.* **2016**, *342*, 27−39.

https://doi.org/10.1021/acscatal.1c04767
ACS Catal. 2022, 12, 633−647